AGU PUBLICATIONS

JGR

Journal of Geophysical Research: Atmospheres

RESEARCH ARTICLE

10.1002/2013JD021417

Key Points:
- A method is introduced to quantify the effects of mixing on age of air
- Mixing mostly leads to additional aging of air, due to recirculation
- The mixing strength is tightly coupled to the residual circulation strength

Correspondence to:
H. Garny,
hella.garny@dlr.de

Citation:
Garny, H., T. Birner, H. Bönisch, and F. Bunzel (2014), The effects of mixing on age of air, *J. Geophys. Res. Atmos.*, *119*, 7015–7034, doi:10.1002/2013JD021417.

Received 22 DEC 2013
Accepted 23 MAY 2014
Accepted article online 28 MAY 2014
Published online 17 JUN 2014

The effects of mixing on age of air

H. Garny[1], T. Birner[2], H. Bönisch[3], and F. Bunzel[4]

[1]Deutsches Zentrum für Luft- und Raumfahrt, Institut für Physik der Atmosphäre, Oberpfaffenhofen, Germany, [2]Department of Atmospheric Science, Colorado State University, Fort Collins, Colorado, USA, [3]Institute for Atmospheric and Environmental Sciences, Goethe University Frankfurt, Frankfurt am Main, Germany, [4]Max Planck Institute for Meteorology, Hamburg, Germany

Abstract Mean age of air (AoA) measures the mean transit time of air parcels along the Brewer-Dobson circulation (BDC) starting from their entry into the stratosphere. AoA is determined both by transport along the residual circulation and by two-way mass exchange (mixing). The relative roles of residual circulation transport and two-way mixing for AoA, and for projected AoA changes are not well understood. Here effects of mixing on AoA are quantified by contrasting AoA with the transit time of hypothetical transport solely by the residual circulation. Based on climate model simulations, we find additional aging by mixing throughout most of the lower stratosphere, except in the extratropical lowermost stratosphere where mixing reduces AoA. We use a simple Lagrangian model to reconstruct the distribution of AoA in the GCM and to illustrate the effects of mixing at different locations in the stratosphere. Predicted future reduction in AoA associated with an intensified BDC is equally due to faster transport along the residual circulation as well as reduced aging by mixing. A tropical leaky pipe model is used to derive a mixing efficiency, measured by the ratio of the two-way mixing mass flux and the net (residual) mass flux across the subtropical boundary. The mixing efficiency remains close to constant in a future climate, suggesting that the strength of two-way mixing is tightly coupled to the strength of the residual circulation in the lower stratosphere. This implies that mixing generally amplifies changes in AoA due to uniform changes in the residual circulation.

1. Introduction

A clear conceptual picture of the stratospheric transport circulation, the Brewer-Dobson circulation (BDC), has evolved over the last decades (reviewed in, e.g., *Butchart* [2014], *Plumb* [2002], and *Shepherd* [2007]). The zonal mean part of this transport circulation can be characterized by mean mass flux as given by the residual mean meridional circulation (residual circulation hereafter; see section 2.2), and by two-way exchange of air masses. The residual circulation consists of upwelling in the tropics, poleward transport and downwelling in middle to high latitudes, as illustrated in Figure 1 (black arrows). Strong two-way mass exchange is caused by breaking planetary waves, leading to strong quasi-horizontal stirring, displacing air masses over thousands of kilometers [*McIntyre and Palmer*, 1984]. Turbulent mixing toward smaller scales and eventually molecular diffusion results in the irreversibility of the displacement of air. The two-way mass exchange resulting from the entire cascade from stirring by planetary waves to turbulent mixing is referred to as "(two-way) mixing" in the context of this work [see also *Shuckburgh and Haynes*, 2003; *Plumb*, 2002]. Enhanced wave breaking leads to strong two-way mixing in the extratropical surf zone [*McIntyre and Palmer*, 1984], illustrated by blue arrows in Figure 1. While the tropics are generally well isolated from the extratropics by the subtropical barrier [e.g., *Trepte and Hitchman*, 1992], two-way mixing across this barrier can occur, for example, due to breaking planetary waves [e.g., *Randel et al.*, 1993] (red arrows in Figure 1).

Stratospheric age of air is defined as the transit time of an air parcel since its entry into the stratosphere [*Hall and Plumb*, 1994]. Thus, age of air is a measure of the integrated effect of all transport processes that affect the pathway of an air parcel through the stratosphere. Mean age of air (AoA) is the first moment of the transit time distribution at a certain location in the stratosphere and is often used to quantify the strength of the transport circulation in the stratosphere (the BDC). It has been long recognized from conceptual model studies that mixing between the tropics and extratropics can increase AoA globally [*Neu and Plumb*, 1999]. The additional aging is caused by the "recirculation" of air parcels through the stratosphere, as illustrated in Figure 1: An air parcel enters the stratosphere (A) and travels along the residual circulation to the extratropics (B). From there, it can be mixed back into the tropics (B to C) and thus recirculates along the residual circulation (C to D). The parcel's age increases steadily while performing multiple circuits through the

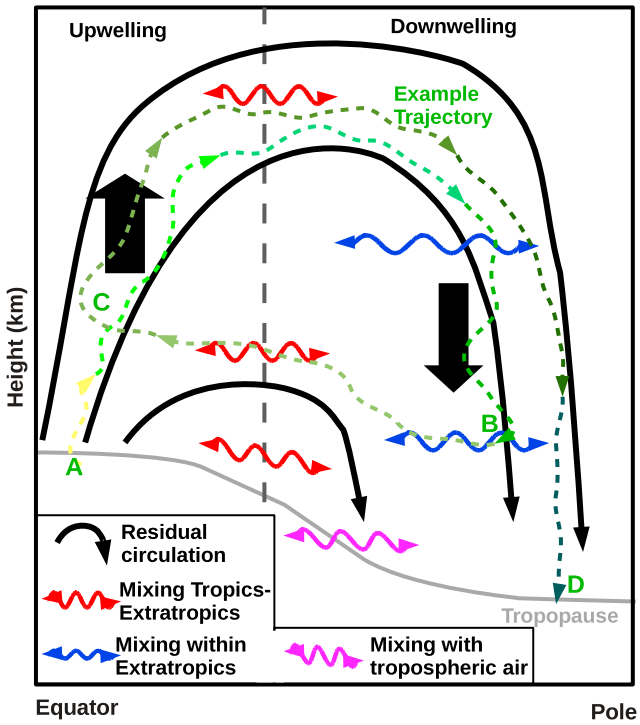

Figure 1. Illustration of stratospheric transport processes (for details, see text).

stratosphere. Thus, the process of *mixing* (transition B to C) affects the air parcel's age as it leads to *recirculation* (C to D). Note that due to the definition of mixing as two-way mass exchange, another air parcel of same mass had to be mixed from C to B at the same time. In the following, we refer to the effect of mixing on AoA as *aging by mixing*.

AoA can be estimated from observations of quasi-passive tracers with monotonically increasing concentrations, such as SF_6 [*Bönisch et al.*, 2009]. *Strahan et al.* [2009] used ascent rates from the observed tropical water vapor tape recorder to estimate tropical modal AoA (i.e., the most probable transit time). The difference of modal AoA to mean AoA was than used to empirically quantify the effects of mixing on AoA. However, it is important to note that it is impossible to directly measure the residual circulation, so that only the integrated effect of all transport processes can be estimated from observations. Therefore, the relationship between the residual circulation and AoA needs to be better understood.

In the light of recent results on trends in the strength of the BDC, the understanding of mechanisms that drive changes in the circulation came into focus. While global models project a strengthened residual circulation in a changing climate, and simultaneously a decrease in AoA [*Butchart et al.*, 2010], evidence of trends in AoA from observational estimates is weak [*Engel et al.*, 2009; *Stiller et al.*, 2012; *Diallo et al.*, 2012; *Bönisch et al.*, 2011]. In models, so far the focus of studies was on the mechanisms for the intensification of the residual circulation [*Garcia and Randel*, 2008; *McLandress and Shepherd*, 2009; *Calvo and Garcia*, 2009; *Shepherd and McLandress*, 2011; *Okamoto et al.*, 2011; *Bunzel and Schmidt*, 2013; *Oberländer et al.*, 2013]. *Austin and Li* [2006] found that empirically, AoA is linearly linked to tropical upwelling. *Li et al.* [2012] investigated changes in age spectra and found that both the modal AoA and the tail of the spectrum contribute to the decrease of mean AoA, concluding that mixing plays a substantial role for the decrease in AoA. However, the relationship between the residual circulation and AoA, and possible impacts of changes in two-way mixing on AoA are not well understood. *Ray et al.* [2010] emphasize that trends in AoA are strongly sensitive to possible changes in two-way mixing between the tropics and extratropics.

In this paper, we seek to gain better understanding of the effects of mixing on AoA. To this end, we use simulations with a general circulation model (GCM) that provides AoA together with consistent information on the residual circulation. The residual circulation transit time, the transit time of hypothetical transport solely by the residual circulation, is obtained as described in section 2 and used in section 3 to quantify the effect of mixing on AoA. To better understand those effects, two conceptual model approaches are used: the tropical leaky pipe (TLP) model (section 4.1), which assumes two columns of well-mixed air (a tropical and an extratropical column), is used to quantify the strength of mixing across the subtropical barrier that is necessary to explain the aging by mixing in the GCM. In addition, a simple Lagrangian random walk model (section 4.2) is used to reconstruct the latitudinal distribution of aging by mixing and to illustrate the effects of mixing at different locations in the stratosphere. To elucidate the role of mixing for long-term changes in AoA and possible coupling of the mixing strength and the residual circulation, three equilibrium climate states are compared in section 5.

2. Methods

2.1. Model Description

The comprehensive GCM used in this study is ECHAM6 [*Stevens et al.*, 2013]. Simulations were performed in the time slice mode, i.e., under stationary boundary conditions, for preindustrial (1860), present-day (1990), and future (2050) climate states. These simulations are referred to as TS1860, TS1990, and TS2050 in the following. For each time slice 50 years were simulated after a spin-up period of 5 years. Prescribed boundary conditions including greenhouse gas concentrations (including also chlorofluorocarbons), sea surface temperatures (SST), sea ice coverage (SIC), ozone distribution, and aerosols were applied to simulate the different climate states. Both SST and SIC input data were taken from the output of coupled atmosphere-ocean GCM simulations performed with ECHAM5 [*Röckner et al.*, 2003] coupled to MPIOM (Max Planck Institute Ocean Model) [*Marsland*, 2003], which were carried out for CMIP3. For the future time slice boundary conditions follow the Representative Concentration Pathways (RCP) 4.5 scenario [*Vuuren et al.*, 2011], except SST and SIC that are taken from a simulations that followed the Special Report on Emissions Scenario (SRES) A1B scenario [*Nakicenovic and Swart*, 2000]. The CMIP5 simulations, which follow the RCP4.5 scenario, were not completed by the start of the experiments used in this study. However, the inconsistency between the SST/SIC data set and the prescribed atmospheric conditions is small as both the SRES A1B and the RCP4.5 scenarios assume steadily rising CO_2 concentrations to levels around 500 ppm in 2050 [*Vuuren et al.*, 2011]. In all simulations the horizontal resolution is T63 (1.9° × 1.9°), while the vertical model domain extends up to 0.01 hPa with 47 levels. For details see *Bunzel and Schmidt* [2013].

2.2. Calculation of Residual Circulation Transit Time and Age of Air

Residual circulation transit times (RCTTs) are calculated following *Birner and Bönisch* [2011]. The principle is based on calculating backward trajectories that are driven by the residual mean meridional and vertical winds. The residual velocities ($\bar{v}^*$, $\bar{w}^*$) are calculated from 6-hourly model output of meridional and vertical winds (v, w) and potential temperature (Θ) as follows [*Andrews et al.*, 1987, equation (3.5.1)]:

$$\bar{v}^* = \bar{v} - \frac{1}{\rho_0}\frac{\partial}{\partial z}\left(\rho_0 \overline{v'\Theta'} / \frac{\partial \Theta_0}{\partial z}\right) \tag{1}$$

$$\bar{w}^* = \bar{w} + \frac{1}{r\cos\phi}\frac{\partial}{\partial \phi}\left(\overline{\cos\phi\, v'\Theta'} / \frac{\partial \Theta_0}{\partial z}\right) \tag{2}$$

Monthly mean velocities are then used to calculate the backward trajectories in the latitude-height plane with a standard fourth-order Runge-Kutta integration. The backward trajectories are initialized on a grid with 35 latitudes (spaced every 5°) and on 10 pressure levels (200, 170, 150, 120, 100, 70, 50, 30, 20, and 10 hPa). The backward trajectories are terminated when they reach the thermal tropopause (calculated following the WMO definition), and the elapsed time is the residual circulation transit time. Trajectories are initialized in the middle of a month, and are calculated backward using the varying residual velocities and tropopause values. RCTTs are calculated for every month of the last 10 years of each time slice simulation. In the following, annual mean climatological values of RCTTs are used (i.e., averaged over 120 values per grid point). As the interannual variability in annual mean AoA is less than 10% everywhere, 10 years of data are sufficient to represent the mean state of the simulations. We focus here on annual mean values as we are mainly interested in mean effects of mixing on long-term changes. For a discussion of the seasonal cycle in RCTT see *Birner and Bönisch* [2011].

In GCM simulations with ECHAM6 a passive tracer is used to derive AoA. Following *Hall and Plumb* [1994] this tracer is initialized in the lowermost model level between 5°S and 5°N with concentrations increasing linearly over time. The time lag in tracer concentrations between a certain grid point in the stratosphere and the tropical tropopause provides an estimation of AoA at this stratospheric grid point. The reference point at the tropical tropopause for age tracer concentrations is set between 10°S and 10°N as the height of the thermal tropopause (i.e., consistent with the RCTT calculations).

3. Effects of Mixing on Age of Air in a GCM

AoA averaged over 10 years from the TS1990 simulation is shown in Figure 2. In addition, the hypothetical age if air was transported only by the residual circulation (RCTT) calculated over the same time period than AoA is shown. The RCTT considerably differs from AoA both in magnitude and structure. While AoA

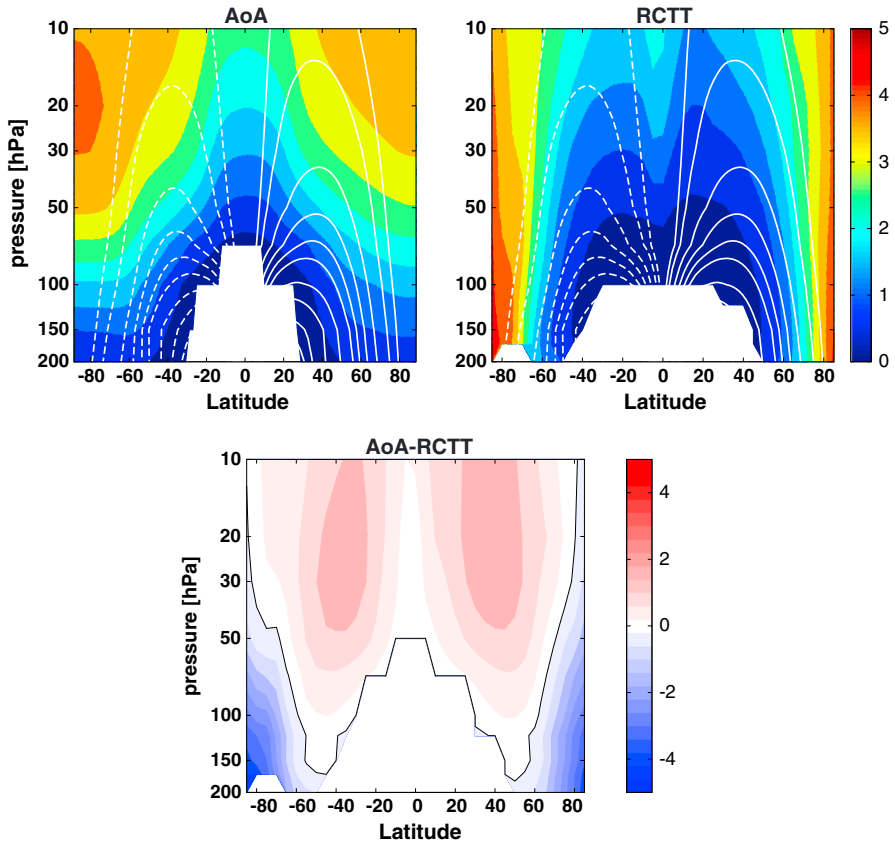

Figure 2. AoA, RCTT, and aging by mixing (the difference AoA-RCTT) from ECHAM6, TS1990, annual mean values averaged over 10 years in units of *years*. (top) The annual mean residual circulation stream function is overlaid (white contours, dashed: negative; solid: positive). (bottom) The thin black line is the zero line.

isolines are orientated quasi-horizontally, RCTT has a strong meridional gradient in particular in middle to high latitudes. In contrast to the distribution of AoA, RCTT clearly follows the structure of the residual mean circulation (white contours in Figure 2). The strong gradient in RCTT from middle to high latitudes marks the different residual circulation branches, as discussed by *Birner and Bönisch* [2011]: The shallow branch consists of upward net mass transport in the (sub)tropics, poleward and downward in midlatitudes, with air mostly remaining below about 70 hPa. The deep branch, on the other hand, consists of upward net mass transport in the deep tropics and downward at high latitudes. The branches are also manifested in distinct regions of wave breaking: the shallow branch is predominantly driven by wave breaking in the subtropical lower stratosphere, while the deep branch is predominantly driven by wave breaking in the vicinity of the polar night jet in the middle stratosphere.

The advantage of global model data is the availability of AoA and consistent with it the residual circulation, and thus RCTT, so that AoA can be compared with those hypothetical transit times. The difference between AoA and RCTT can be interpreted as the modification of the transit time following net air mass transport by additional processes, including quasi-horizontal two-way mixing, but also vertical diffusion or any (numerical) uncertainties in the calculation of AoA and RCTT. The representation of advection in the model certainly affects the strength of the simulated two-way mixing mass flux, so that numerical diffusion is implicitly included in our definition of two-way mixing (this is further discussed in section 6). We assume in the following that other numerical uncertainties (e.g., in the calculation of RCTT) are small and thus that the difference between AoA and RCTT is caused by two-way mixing. We refer to the difference between AoA and RCTT as *aging by mixing*.

In most of the stratosphere, air is older than if it was only transported along the residual circulation (see Figure 2, bottom). Aging by mixing maximizes in midlatitudes and increases with height. In the lowermost

extratropical stratosphere and close to the poles, mixing reduces transit times—here air is younger than for purely residual transport.

The distribution of aging by mixing does not necessarily resemble the distribution of mixing strength, measured, for example, by effective diffusivity [*Haynes and Shuckburgh*, 2000]. Neither does aging by mixing maximize in regions of wave breaking. As will be shown in section 4, aging by mixing at one particular point in the stratosphere can be induced by mixing remote to this point. Furthermore, mixing in different regions of the atmosphere has varying impacts on AoA. Therefore, it cannot be expected that the effect of mixing on AoA (i.e., aging by mixing) is locally related to the mixing strength.

4. Effects of Mixing on Age of Air in Conceptual Models

4.1. The Tropical Leaky Pipe Model

4.1.1. Formulation of the Tropical Leaky Pipe Model

The tropical leaky pipe (TLP) model, described in *Neu and Plumb* [1999] (NP99 in the following), divides the stratosphere into the tropical pipe and the well-mixed surf zones of the southern and northern hemisphere. It is assumed that (1) mixing within the surf zones is fast compared to mixing across the boundary and (2) the surf zone extends all the way to the pole (i.e., the polar regions with their seasonal barrier are neglected). Thus, the model is essentially one-dimensional (vertical coordinate) with three columns that can interact. The tropical pipe corresponds to the upwelling region (see Figure 1), and the surf zones to the downwelling region. Vertical motion within each region is prescribed. Furthermore, horizontal exchange between the tropics and the surf zones is allowed. We further make the following simplifications to the model: First, vertical diffusion is neglected. In NP99 it was shown that AoA using the vertical diffusivity as reported by *Sparling et al.* [1997] is very similar to AoA in the nondiffusive case, except close to the extratropical tropopause. Second, we assume that the hemispheres are symmetric (i.e., the properties of the northern surf zone equal those of the southern surf zone). With these simplifications, the formulation of the tracer budget equations for a passive tracer with mixing ratio σ in the tropics (T) and surf zones (SZ) and with sources S_T and S_{SZ} are given by

$$\frac{\partial \sigma_T}{\partial t} - S_T = -w_T \frac{\partial \sigma_T}{\partial z} - \frac{1}{\alpha}\epsilon\lambda(\sigma_T - \sigma_{SZ}) \tag{3}$$

$$\frac{\partial \sigma_{SZ}}{\partial t} - S_{SZ} = -w_{SZ} \frac{\partial \sigma_{SZ}}{\partial z} + (\epsilon + 1)\lambda(\sigma_T - \sigma_{SZ}) \tag{4}$$

where w_T and w_{SZ} are the vertical velocities in the tropics and surf zones, respectively, and α is defined as the ratio of tropical to the extratropical mass ($\alpha = M_T/(2M_{SZ})$, where M_{SZ} is the mass in either hemisphere, as they are assumed to be symmetric). The horizontal transport between tropics and extratropics is described by two relaxation factors λ and ϵ. The factor λ is defined as the horizontal transport that is determined by mass continuity by the prescribed vertical velocities (i.e., $\partial_y \bar{v}^* = -1/\rho\, \partial_z(\rho \bar{w}^*)$). Following NP99, λ is calculated as

$$\lambda = -\frac{1}{M_T}\frac{\partial(M_T w_T)}{\partial z} \tag{5}$$

The factor ϵ, on the other hand, describes the two-way mass exchange (i.e., what we describe as mixing) and can be chosen freely. ϵ is defined as the ratio of the mass flow from the surf zones to the tropics to the net mass flux between tropics and the surf zones. The net mass flux is the horizontal motion that is determined by mass continuity via the prescribed vertical motion (given by λ), and corresponds to transport by $\bar{v}^*$. If $\epsilon = 0$, there is no mixing, and if $\epsilon = 2$, the mass flow due to mixing in either direction is twice as large as the net mass flow. We will refer to ϵ in the following as *mixing efficiency*.

If it is further assumed that w_T and ϵ are constant with height, a simple analytical solution for the tropical age (Γ_T) and age in the surf zones (Γ_{SZ}) in the TLP model can be formulated (for the derivation see section 3 in NP99):

$$\Gamma_T = \frac{\alpha + \epsilon(\alpha + 1)}{\alpha w_T}(z - z_T) \tag{6}$$

$$\Gamma_{SZ} = \frac{\alpha + \epsilon(\alpha + 1)}{\alpha w_T}(z - z_T) + \frac{(1 + \alpha)}{\lambda} \tag{7}$$

The vertical coordinate z is the equivalent height above the extratropical tropopause ($z = 0$), and z is parallel to age isopleth (see NP99). The height of the tropical tropopause is z_T.

4.1.2. Aging by Mixing in the Tropical Leaky Pipe Model

The diagnostics AoA and RCTT can be described with the TLP model such that AoA is the full age with mixing efficiency ϵ (Γ^{ϵ}), while RCTT is the solution with $\epsilon = 0$ (Γ^{0}). From equation (6) it follows that aging by mixing in the tropics (A^{T}_{mix}) equals

$$A^{T}_{\mathrm{mix}} = \Gamma^{\epsilon}_{T} - \Gamma^{0}_{T} = \epsilon(1 + \frac{1}{\alpha})\frac{z - z_T}{w_T} \tag{8}$$

Aging by mixing in the surf zones calculated as $\Gamma^{\epsilon}_{\mathrm{SZ}} - \Gamma^{0}_{\mathrm{SZ}}$ equals aging by mixing in the tropics, i.e., a certain mixing efficiency causes air to age as much in the tropics as in the extratropics. A_{mix} is always positive above the tropical tropopause and negative below, in agreement with the result from the GCM that mixing leads to an increase of AoA in most of the stratosphere and a decrease in the extratropical lowermost stratosphere.

According to the TLP formulation, aging by mixing is not only a function of the mixing efficiency but also of the vertical velocity—or in other words, the residual circulation strength. A_{mix} is proportional to ϵ (i.e., the higher the mixing efficiency, the larger aging by mixing) but indirectly proportional to w_T (i.e., the larger the vertical velocity, the smaller the additional aging due to mixing). The increase of aging by mixing with the mixing efficiency was explained in NP99 by the recirculation' effect, as was described in section 1: Mixing between young tropical air and older air in the surf zones adds older air into the tropics. This older air recirculates upward in the tropical pipe and eventually back into the surf zone, thus eventually conducting multiple circuits through the stratosphere. Thereby, older air is added both in the tropics and surf zones, aging the air in both regions by the same amount. The recirculation will be examined further with a Lagrangian random walk model in section 4.2.

While a higher mixing efficiency causes more air parcels to recirculate, thereby increasing aging by mixing, the velocity w_T controls the speed of the recirculation. If w_T increases, the additional circuits air parcels travel take less time and aging by mixing decreases. Thus, even under a constant mixing efficiency, aging by mixing can change if the speed of the residual circulation changes. In principle, an increase in the vertical velocity w_T could be counteracted by changes in the mixing efficiency ϵ in a way that AoA remains unaffected. However, as will be discussed in section 5, mixing by wave breaking is not independent of residual transport.

4.1.3. Mixing Efficiency in the GCM Derived With the Tropical Leaky Pipe Model

The TLP model in the formulation as described above has two free parameters that can be chosen: the tropical vertical velocity w_T and the mixing efficiency ϵ. The vertical velocity can be diagnosed easily from the GCM data as the mean $\bar{w}^{*}$ in the tropics. We choose a latitude band of 30°S–30°N as tropical pipe, as these latitudes capture the approximate region of upwelling best (the turnaround latitudes lie between 25–40°N/S, depending on height).

The analytical solution of the TLP model with a height dependent vertical velocity $w_T(z)$ (see equations (9) and (10) of NP99) for tropical AoA is:

$$\Gamma_T(z) = \int_{z_T}^{z} \frac{1}{w_T(z')}\mathrm{d}z' + \epsilon\frac{(\alpha+1)}{\alpha}\left(\int_{z_T}^{z} \frac{1}{w_T(z')}\mathrm{d}z' + H(\frac{1}{w_T(z)} - \frac{1}{w_T(z_T)}\right) \tag{9}$$

where H is the scale height (7 km). In the following we will approximate the mean tropical profiles of AoA and RCTT using this solution of the TLP model. RCTT can be calculated from the TLP model using tropical vertical velocities from the GCM as input and setting ϵ to zero. As shown in Figure 3, the tropical RCTT from the GCM (solid blue line) are reasonably well reproduced with the TLP Model (dashed blue line). Deviations are $\leq$ 10% above 50 hPa and $\leq$ 33% below; the high relative deviation at the lowest level is due to the small absolute value of transit time here.

For given vertical velocities, the difference between AoA and RCTT depends only on the mixing efficiency ϵ. Thus, ϵ can be derived from the tropical AoA and RCTT profiles as the best fit of the TLP model to the GCM profiles. The best fit over all layers in the lower stratosphere (tropopause to 10 hPa) is obtained with a mixing efficiency of $\epsilon = 0.32$ for the TS1990 simulation. Thus, given the definition of ϵ in section 4.1.1, the mixing mass flux across the subtropical barrier is about a third as strong as the net mass flux into the extratropics. The result for ϵ is robust (within 10%) for latitude bands within the range of the border of the tropical pipe (i.e., between 25 and 40°N/S). The fit with the TLP model reproduces tropical AoA from the GCM reasonably well, mostly with deviations $\leq$ 10% expect around 70 hPa, where deviations are larger (30%). Fitting the

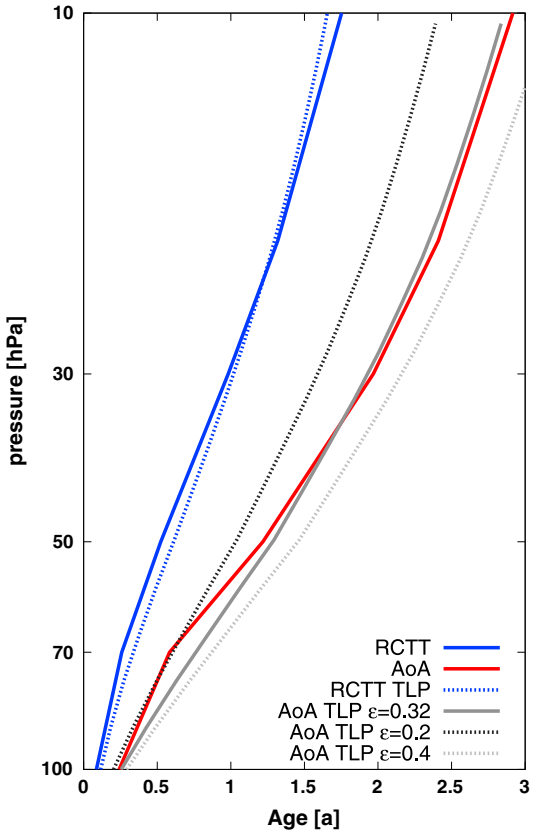

Figure 3. Tropical mean (30°S-30°N) profiles of RCTT (blue) and AoA (red) from the GCM (TS1990) together with the results of the TLP model for RCTT (blue dotted) and AoA with $\epsilon = 0.2$ (dark gray dashed), $\epsilon = 0.4$ (light gray dashed) and the best fit to the GCM data with $\epsilon = 0.32$ (gray solid).

TLP model only at levels above 70 hPa does, however, result in only slight changes of the mixing efficiency (0.33 instead of 0.32) and further results are not affected. The larger deviations in the lower levels might be caused either by the simplified assumption of a constant width of the tropical pipe with height (close to the tropopause, the tropical pipe narrows) or might indicate that mixing efficiencies in the shallow branch differ from those in the deep branch of the BDC. For the lower levels, a smaller mixing efficiency of about 0.2 results in a better fit to AoA.

As discussed above, AoA increases with the mixing efficiency, as shown by the dashed lines in Figure 3. These cases would represent a stronger or weaker relative mixing mass flux compared to the net mass flux. How the net and mixing mass flux are related is further discussed in section 5.

4.2. A Lagrangian Random Walk Model of Mixing Effects

The TLP model used in the last section is suitable to quantify effects of mixing across the subtropical barrier on the tropical and extratropical mean AoA profiles. However, the latitudinal structure of aging by mixing found in the GCM cannot be captured by the TLP model due to its setup. To examine the causes for the distribution of aging by mixing and to analyze the role of mixing at different locations in the stratosphere, we developed a simple Lagrangian transport model (section 4.2.2 and Appendix A). We start by illustrating effects of mixing on AoA in the Lagrangian framework using simple conceptual experiments.

4.2.1. Conceptual Experiments on Recirculation and Mixing Effects

The TLP model predicts that tropical-extratropical mixing of a certain strength increases AoA as much in the tropics as in the extratropics through the effect of recirculation of air parcels (equation (6); also discussed in NP99). This effect can be illustrated with the following simple Lagrangian experiment:

We use a trajectory calculated from residual velocities (see Figure 4a). Along the trajectories, points that are equally spaced in time (with $\Delta t = 5$ days) are defined, and each point is assigned with 100 air parcels of equal mass. Air parcels are advected along the trajectories, and their transit time increases as they do so. Two-way mixing is included in the model by instantaneously exchanging a given fraction of randomly chosen air parcels between predefined mixing points. As mixing is likely to take place along isentropic surfaces in the real atmosphere, we use the intersections of the trajectories with isentropic surfaces as mixing points. For this first simple experiment we chose the 380 K level and exchange an arbitrarily chosen fraction of $\mu = 10\%$ of randomly selected parcels between the tropical and the extratropical mixing point. The random exchange of air parcels essentially results in a random walk of the air parcels.

When running the model for a sufficient amount of time, a new equilibrium AoA is reached that is greater than AoA without mixing at all locations between the two mixing points (compare red and black lines in Figure 4c), as was predicted by the TLP model. It can be clearly seen from the age spectrum at 50°N that the additional aging is caused by in-mixing of old air from the extratropics to the tropics, which subsequently recirculates along the deep branch. Below the extratropical mixing point, AoA is unchanged when mixing is included. This simple experiment illustrates that this is due to a cancellation of old recirculating air and young air that was mixed in from the tropical lower stratosphere: the age spectrum at 85°N (Figure 4c) shows that as much very young (less than 1 year) air parcels are found as old air parcels, which were mixed

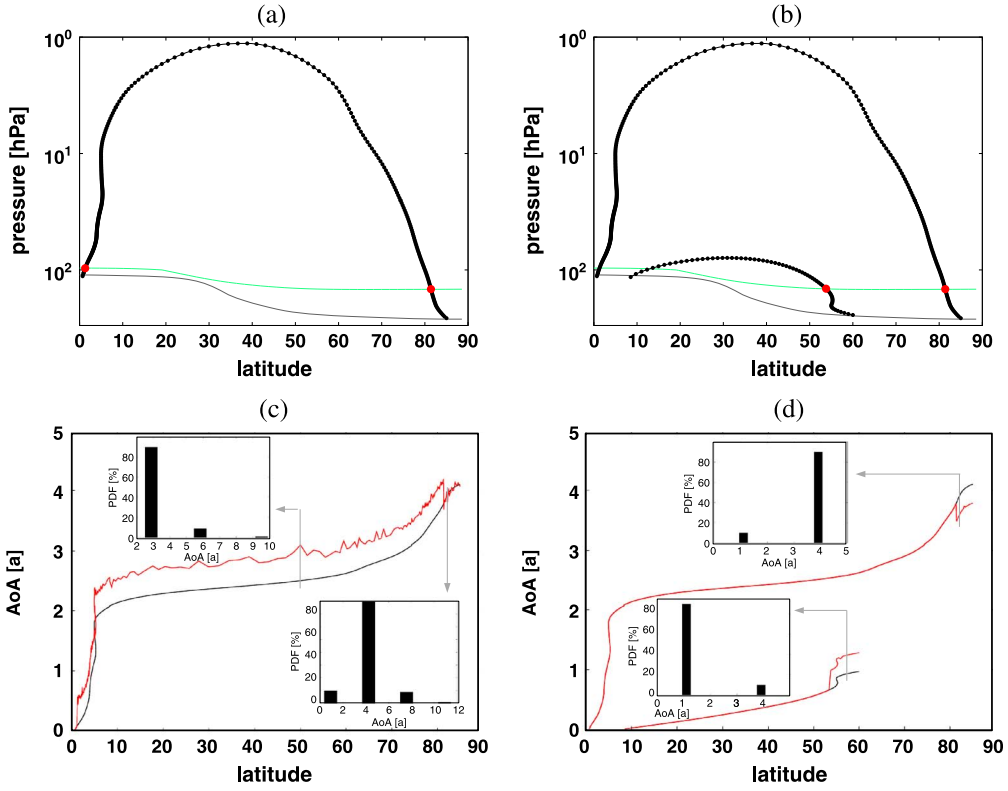

Figure 4. Illustration of the effects of mixing on age. (a, c) Mixing of tropical and extratropical air from the deep circulation branch. (b, d) Mixing of extratropical air from the shallow and the deep branch. Figures 4a and 4b show the example trajectories and the mixing points at 380 K (red dots, 380 K isentrope as green line, tropopause as thin black line). Figures 4c and 4d show the mean age along the trajectory (here shown as function of latitude) without mixing (black) and after integration over 10 times the trajectory length (red). Inlets show age spectra at indicated points.

to the tropics, recirculate along the trajectory and eventually reach the region below the extratropical mixing point. They have aged exactly the age difference between the tropical and extratropical mixing point and thus exactly compensate for the younger tropical air.

Thus, mixing between the tropics and extratropics at a certain level only affects air above this level, and the additional aging depends only on the age difference between the tropics and extratropics. It follows that mixing at lower levels will have an overall larger impact on AoA than mixing at higher levels. Note that this is consistent with the TLP model, which predicts that mixing leads to aging of air that is equally strong in the tropics as in the extratropics (see equation (6)). As mixing at a certain level affects tropical AoA only above this level, it follows that also extratropical AoA must be unaffected by mixing below the level of mixing.

In the TLP model, the effects of mixing across the subtropical barrier are examined, while mixing within the extratropics is assumed to be very strong. This is a valid assumption as long as the strength of mixing within the extratropics does not affect the extratropical mean AoA profile (and thus not tropical mean AoA, according to the arguments above). In the following, we illustrate with the simple Lagrangian model that mixing within the extratropics can have an effect on extratropical mean AoA given that air parcels take different pathways, for example, along the different branches of the BDC. However, this effect is small compared to mixing across the subtropical barrier. We include a second trajectory that represents the shallow branch of the circulation and terminates at the tropopause at 60°N (Figure 4b). A fraction of $\mu = 10\%$ of the air parcels are mixed between the extratropical intersects of the 380 K isentropic level and the two trajectories, i.e., between about 55°N and 80°N. Mixing within the extratropics adds younger air to the lower part of the deep branch trajectory, and older air to the shallow branch trajectory (Figure 4d), thereby flattening the age gradient in the extratropics. Thus, mixing within the extratropics has a strong local effect. The mean extratropical AoA profile can be affected by mixing in case the remaining time of the mixed air parcels in the stratosphere differs. Such a difference in the remaining time can occur essentially depending on the shape

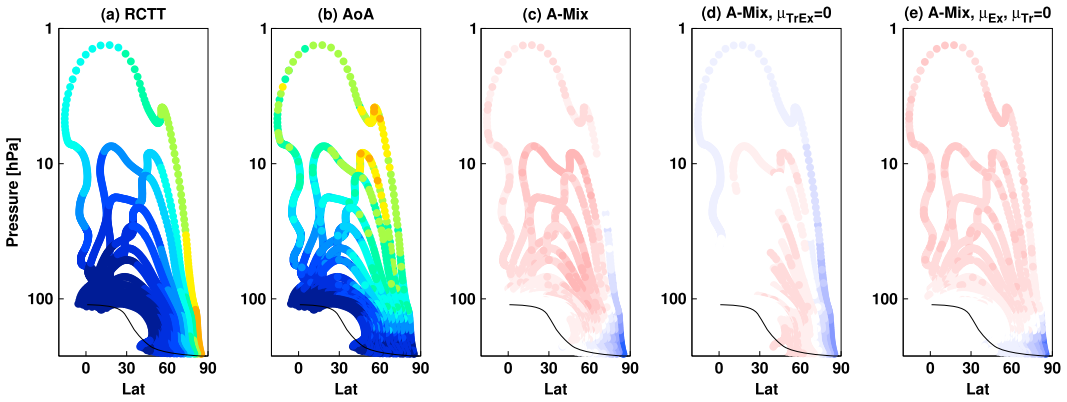

Figure 5. (a) RCTT, (b) AoA, and (c) Aging by mixing simulated with the Lagrangian random walk model using 20 trajectories. (d) Aging by mixing for mixing only within the tropics and within the extratropics. (e) Aging by mixing for mixing only between tropics and extratropics. Color shading as in Figure 2.

of the circulation and the slope of the tropopause. For the example of mixing at 380 K, a small decrease in AoA averaged over all air parcels is found to be induced by mixing. Depending on the altitude of mixing, the net effect on AoA can be positive or negative but is never larger than a few percent in the current example. For comparison, mixing of the same strength between tropics and extratropics has a net effect on AoA of almost 50%. As the difference of the remaining time in the stratosphere is much smaller for air parcels located in the extratropics compared to parcels mixed between tropics and extratropics this is expected. However, as mixing in the extratropics has a strong local effect, we will investigate in the following how the distribution of aging by mixing is influenced by mixing at different locations.

4.2.2. Distribution of Aging by Mixing

We extend the Lagrangian model to a set of 20 trajectories that terminate between 40° and 85°N at the tropopause. This set of 20 trajectories represents mean transport along different branches of the residual circulation in the Northern Hemisphere. The transit times along the trajectories are shown in Figure 5a.

Mixing points are defined as the intersects of trajectories with 20 isentropic levels between 340 K and 2000 K. The calculation of mixing between all the intersects on one isentrope would become quickly excessive when adding more trajectories (0.5*M(M-1) interchanges for M intersects). Thus, air parcels are grouped into tropical and extratropical parcels, and mixing is performed within and between those groups. Thus, three mixing events are possible at each isentropic level: (1) mixing within the tropics, (2) mixing of tropical and extratropical air, and (3) mixing within the extratropics. For each class of mixing operation, a height dependent mixing strength (μ_{Tr}, μ_{TrEx}, and μ_{Ex}, respectively) is prescribed as follows: mixing within the tropics and within the extratropics is set to $\mu_{Ex} = \mu_{Tr} = 0.25$. The model is not sensitive to the choice of μ_{Tr}. Mean profiles are also not sensitive to μ_{Ex}, and it is set to best resemble the latitudinal distribution of AoA. The critical parameter is the mixing strength between tropics and extratropics, μ_{TrEx}. We set the tropical-extratropical mixing parameter by assuming that the two-way mixing mass flux is proportional to the net mass flux, which is a realistic assumption as will be shown in section 5. The ratio of two-way mass flux to net mass flux is set to the mixing efficiency as calculated with the TLP model fit (section 4.1). Details on the settings of the Lagrangian model and sensitivities to those settings can be found in Appendix A.

AoA after an integration over 10*N time steps (where N is the number of time steps it takes an air parcels to travel along the longest trajectory) is shown in Figure 5b. Mixing leads to additional aging of air in most of the stratosphere, only in the high latitude lowermost stratosphere age decreases due to mixing. The profiles of tropical and extratropical mean RCTT and AoA from the simple Lagrangian model agree reasonably well with the results from the GCM (Figure 6), and so does the distribution of "aging by mixing" (Figure 5c). The Lagrangian model broadly reproduces the mean latitudinal distribution of AoA and aging by mixing (Figure 7), even though the maximum in aging by mixing is shifted by about 10° poleward compared to the GCM. Since the Lagrangian model is a very simplified representation of transport through the stratosphere, an exact quantitative replication of AoA in the GCM should not be expected. However, general qualitative features of aging by mixing are well captured. Therefore, we can use this idealized model to improve the conceptual understanding of the effects mixing at different locations can have on AoA.

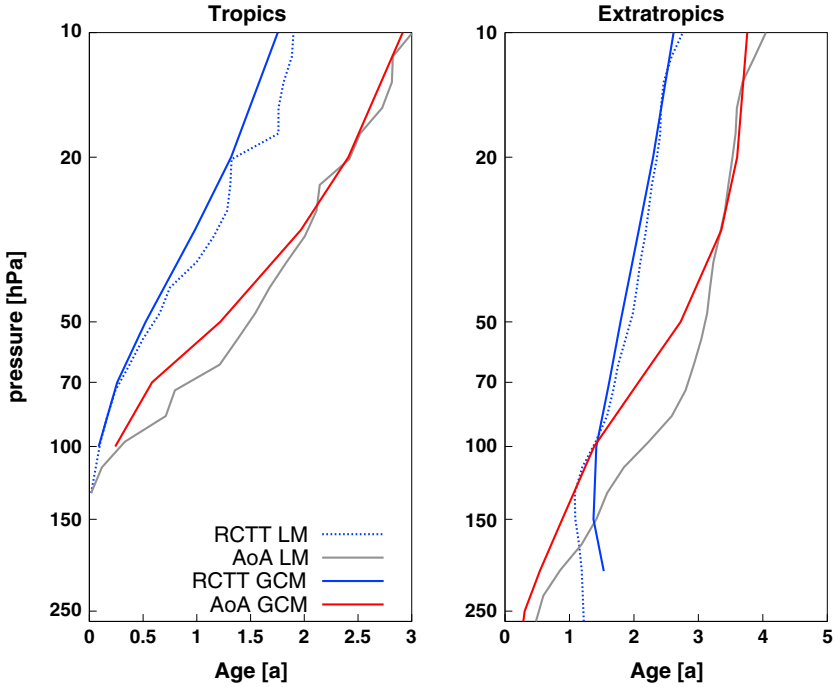

Figure 6. Tropical (0–30°N) and extratropical (35–90°N) mean profiles of RCTT and AoA from the GCM (blue and red solid) and the Lagrangian random walk model using 20 trajectories (blue dashed and gray).

Figure 5 contrasts aging by mixing from the full integration to cases in which mixing is applied (1) only within the tropics and the extratropics (Figure 5d) and (2) only between the tropics and extratropics (Figure 5e). As discussed in section 4.2.1, mixing within the extratropics has a strong local effect and flattens the age gradient, but tropical-extratropical mixing causes an increase in AoA in the entire

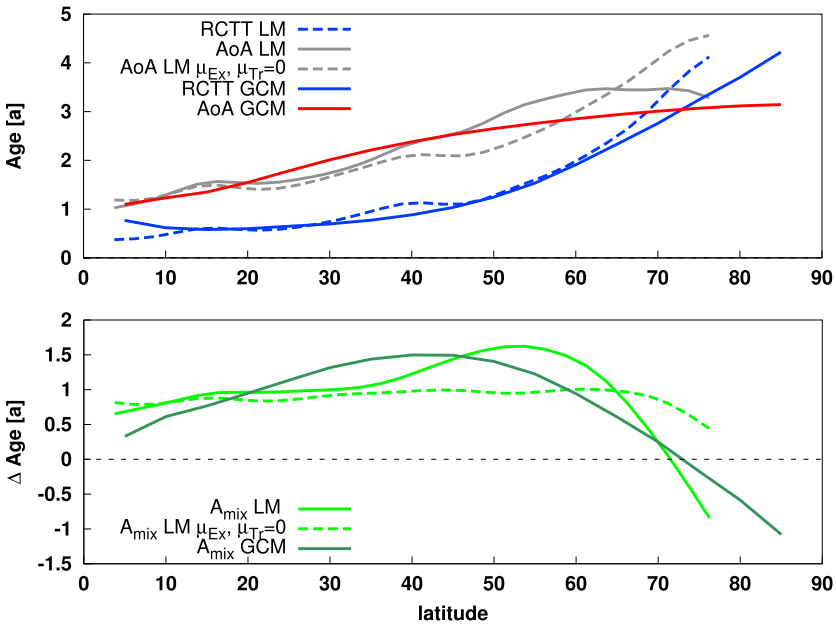

Figure 7. (top) Mean latitudinal distribution averaged over 70–10 hPa of RCTT (solid blue) and AoA (solid red) from the GCM and the Lagrangian random walk model using 20 trajectories (RCTT: blue dashed, AoA: gray). (bottom) Aging by mixing (A_{mix} = AoA − RCTT) from the GCM (dark green) and the Lagrangian model (light green). In addition, AoA and aging by mixing from the Lagrangian random walk model with no mixing within the tropics and within the extratropics is shown ((top) AoA: gray dashed, (bottom) aging by mixing: green dashed).

Table 1. Global Mean AoA and Aging by Mixing (in Years) for Different Cases Calculated With the Lagrangian Random Walk Model: Integration Without Mixing (No Mixing), Full Integration With Base Parameter Settings (Base), Without Mixing Between Tropics and Extratropics ($\mu_{TrEx} = 0$), and Without Mixing Within the Extratropics and Tropics ($\mu_{Ex}, \mu_{Tr} = 0$)[a]

	No Mixing	Base	$\mu_{\mathrm{TrEx}} = 0$	$\mu_{\mathrm{Ex}}, \mu_{\mathrm{Tr}} = 0$	$\mu_{\mathrm{tropo}} = 0$	$\mu_{\mathrm{TrEx}}^{\Theta>500K} = 0$	$\mu_{\mathrm{TrEx}}^{\Theta<500K} = 0$
GM AoA	1.25	1.69	1.30	1.66	1.84	1.61	1.32
GM A_{Mix}	0.0	0.44	0.05	0.41	0.59	0.36	0.07

[a]The case $\mu_{\mathrm{tropo}} = 0$ refers to setting mixing between the tropics and extratropics below the tropical tropopause to zero (i.e., no in-mixing of tropospheric air), and in the cases $\mu_{\mathrm{TrEx}}^{\Theta>500K} = 0$ and $\mu_{\mathrm{TrEx}}^{\Theta<500K} = 0$ tropical-extratropical mixing above and below 500 K is set to zero, respectively.

stratosphere above the level of mixing. Mixing within the tropics has almost no effect, as the gradient in RCTT is small in the tropics. In the mean over all air parcels (global mean), AoA increases from 1.25 to 1.69 years between the case without mixing and the full integration (Table 1). This increase is almost entirely caused by tropical-extratropical mixing, while mixing within the tropics and extratropics has a minor effect, both in the global mean (Table 1, cases $\mu_{\mathrm{TrEx}} = 0$ and $\mu_{\mathrm{Ex}}, \mu_{\mathrm{Tr}} = 0$), and for tropical and extratropical mean profiles (Figure 8). The increase of global mean AoA would be even higher by about 35% if in-mixing of tropospheric air in the lowermost stratosphere is neglected, as verified by an integration in which tropical-extratropical mixing below the tropical tropopause is set to zero ($\mu_{\mathrm{tropo}} = 0$ in Table 1 and Figure 8).

Mixing within the extratropics does, however, affect the latitudinal distribution of aging by mixing. As shown in Figure 7, aging by mixing is nearly constant at all latitudes for the case with only mixing across the subtropical barrier, consistent with the prediction by the TLP model. Only when including mixing within the extratropics, the maximum of aging by mixing in midlatitudes, and the negative values at high latitudes can be reproduced by the Lagrangian model. Since the tropical and extratropical mean profiles are, however,

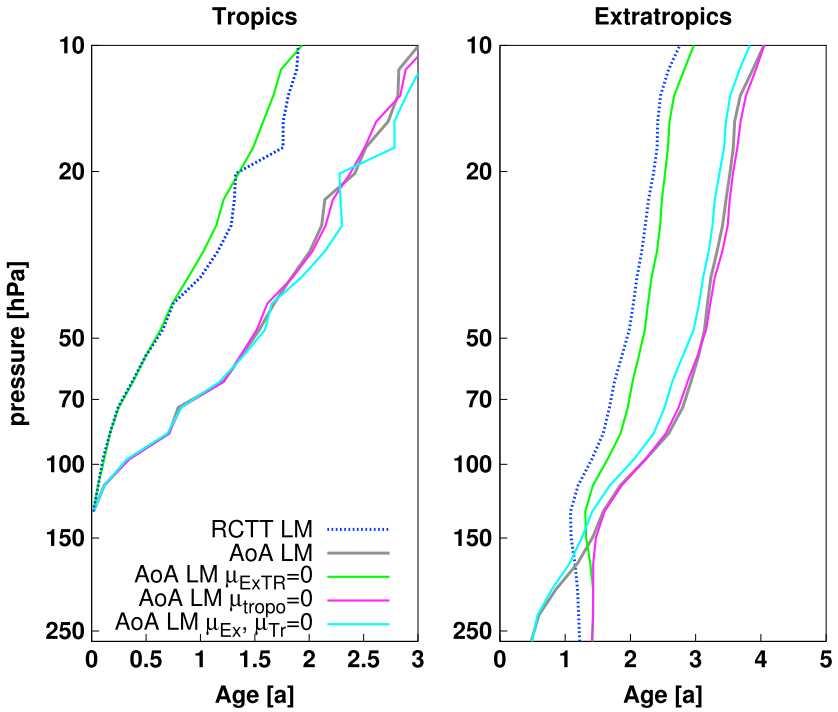

Figure 8. RCTT and AoA from the Lagrangian random walk model as in Figure 6 together with profiles for sensitivity runs with the Lagrangian model without mixing between tropics and extratropics in the entire domain ($\mu_{\mathrm{ExTR}} = 0$, green), without mixing in the lowermost stratosphere (i.e., no mixing below the tropical tropopause, $\mu_{\mathrm{tropo}} = 0$; magenta), and without mixing within the tropics and extratropics ($\mu_{\mathrm{Ex}} = 0$, light blue).

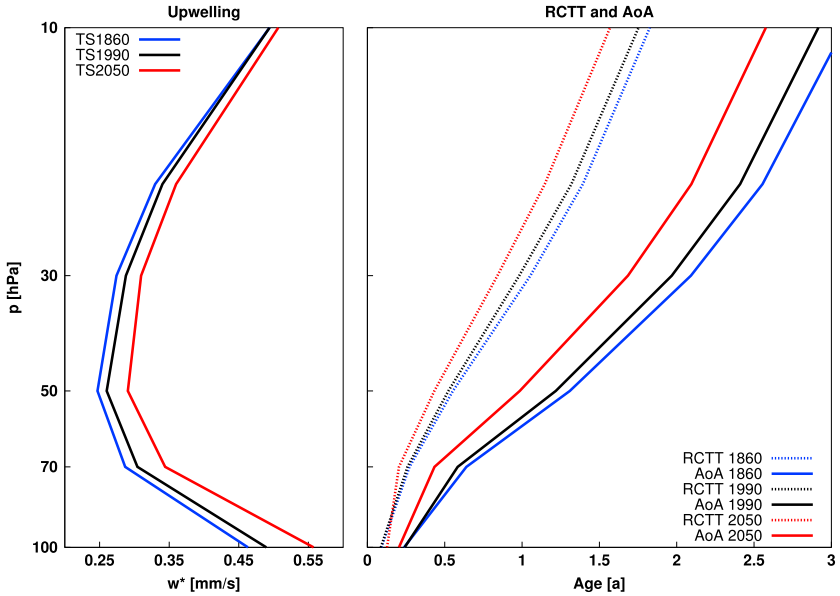

Figure 9. (left) Tropical mean (30°S–30°N) vertical residual velocity from the simulations representing 1860 (blue), 1990 (black), and 2050 (red). (right) Tropical mean (30°S–30°N) RCTT (dotted) and AoA (solid) from the GCM for the three simulations.

not affected by mixing within those regions, applying the TLP model equations to the mean profiles from the GCM appears to be a valid approach.

The role of mixing at different heights is further examined by integrations in which tropical-extratropical mixing is only permitted below or above 500 K. The global AoA increase is far larger for mixing at lower altitudes than for mixing above 500 K (Table 1). Since mixing at a certain level affects AoA only above this level, it can be expected that mixing at lower levels results in an overall greater response in AoA.

The findings with the simple Lagrangian random walk model suggest that the distribution of aging by mixing in the GCM may be explained as follows: the decrease of AoA in the lowermost stratosphere is caused by in-mixing of tropospheric air. The decrease at high latitudes above about 100 hPa, on the other hand, results from mixing within the extratropics, which flattens the gradient in AoA. The general increase in AoA due to mixing is caused by mixing between tropics and extratropics. Tropical-extratropical mixing at a certain levels affects AoA above this level—or, to put it the other way round, AoA at a certain level is influenced by mixing at all levels below. Thus, the higher up, the more mixing levels can contribute to aging by mixing. Therefore, aging by mixing increases with height.

5. Coupling of Mixing and Residual Transport

5.1. Mixing Efficiency in the GCM for Different Climate States

The residual circulation is mechanically driven by the momentum deposition of breaking waves [*Haynes et al.*, 1991]. These are represented in GCMs both by resolved planetary and synoptic scale waves and by parametrized small-scale gravity waves. The two-way mixing mass flux can as well be expected to be linked to wave breaking, which results in strong stirring [*Haynes and Shuckburgh*, 2000]. As discussed in the last section, AoA is controlled both by the residual circulation and by the strength of the two-way mixing mass flux. However, as the two processes are known not to be independent, we want to investigate in this section how they are coupled. To this end, we compare three equilibrium climate states in the model, representative of the mean climate in the 1860s, the 1990s, and the 2050s.

The residual circulation (measured by tropical mean $\bar{w}^*$) is slightly enhanced in 1990 compared to 1860 and even more so in 2050 (Figure 9, left). Consequently, RCTT decreases from 1860 to 2050, and so does AoA (Figure 9 right). In Figure 10, mean tropical AoA at 20 hPa is plotted against mean tropical RCTT for the three simulations. This Figure shows not only that AoA and RCTT both decrease in a warmer climate but also that the ratio AoA/RCTT remains approximately constant (i.e., they lie on a straight line extending through zero). Thus, mixing amplifies changes in AoA, with an about twice as large decrease in AoA than in RCTT both

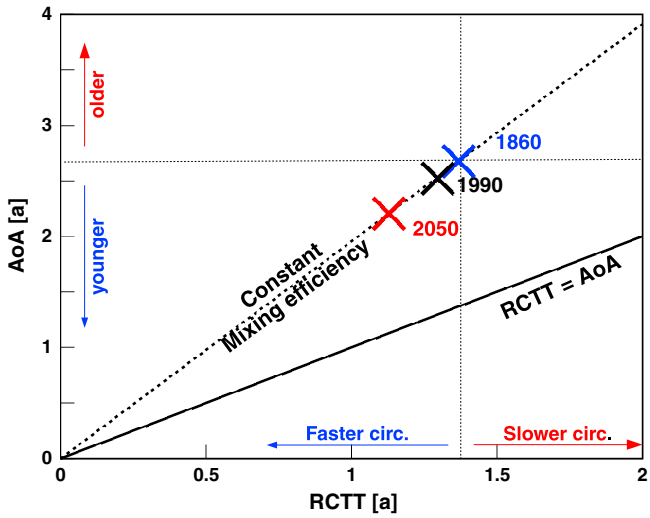

Figure 10. Tropical mean AoA plotted against tropical mean RCTT at 20 hPa from the 1860 (blue), 1990 (black), and 2050 (red) simulation.

for the difference between the TS1860 and TS1990 simulations and between TS1990 and TS2050. In other words, the relative aging of air by mixing remains approximately constant.

For the solution of the TLP model with a height-independent vertical velocity w_T, the ratio AoA to RCTT equals $\Gamma_T^{\epsilon}/\Gamma_T^0 = 1 + \epsilon(1 + \frac{1}{\alpha})$ (see equation (6)), which depends only on the mixing efficiency ϵ. The nearly constant ratio therefore indicates that the mixing efficiency does not change between the simulations. This is confirmed when deriving the mixing efficiency from the profiles of AoA and RCTT for the solution with height-depended $w_T(z)$ as best fit (as in section 4.1): For all three climate states a mixing efficiency of $\epsilon = 0.32$ is obtained. The TLP model with this mixing efficiency describes the change in AoA and RCTT between the climate states well (within 10% at all levels).

The mixing efficiency ϵ is defined as the ratio of the two-way mixing mass flux to the net mass flux. Thus, a constant ϵ for all three climate states corresponds to changes in the two-way mixing mass flux that are proportional to those in the net mass flux. In other words, the results indicate that stronger wave driving of the residual circulation, which drive the enhanced net mass flux [*Bunzel and Schmidt*, 2013], causes more two-way mixing that results in an equally strong enhancement in the two-way mixing mass flux.

Overall, the nearly constant mixing efficiency is equivalent to nearly constant relative aging by mixing. Thus, the decrease in absolute aging by mixing is entirely driven by the strengthened residual circulation: Aging by mixing is indirectly proportional to the residual circulation strength (measured by $\bar{w}^*$; see equation (8)). The stronger residual circulation also causes the recirculation to speed up: the additional transit time an air parcels ages while recirculating is reduced. In other words, the decrease in AoA due to the increase in the residual circulation is amplified by mixing effects, which are, according to this study, tightly coupled to the residual circulation changes.

5.2. PV Gradients

Insight into the relation between the wave forcing, residual circulation strength, and mixing strength can be gained by considering the transformed Eulerian mean zonal momentum equation. In isentropic coordinates, the zonal momentum equation for adiabatic, inviscid flow under steady state can be written as (derived from *Andrews et al.* [1987, equation (3.9.9)] and *Plumb* [2002]):

$$-\bar{v}^*\bar{P}^* = \overline{\hat{v}\hat{P}}^* \tag{10}$$

Here v is the meridional velocity on isentropic levels and P the PV. The zonal average weighted by the isentropic density is denoted by $\bar{x}^*$ and $\hat{x}$ the deviation from $\bar{x}^*$. According to this relation, transport of mean PV by the zonal mean circulation is balanced by eddy fluxes of PV.

Using a flux-gradient relationship for the eddy PV flux, i.e., $\overline{\hat{v}\hat{P}}^* = -K_{\mathrm{mix}}\bar{P}_y^*$ (with diffusivity coefficient K_{mix}), we obtain

$$\bar{v}^*\bar{P}^* = K_{\mathrm{mix}}\bar{P}_y^* \tag{11}$$

Furthermore, by setting the Diffusivity to a mixing velocity scale times a horizontal mixing length scale ($K_{\mathrm{mix}} \sim \overline{v_{\mathrm{mix}}} * L$), the ratio of the diffusive, or "mixing" velocity to the mean meridional velocity is given by

$$\frac{\overline{v_{\mathrm{mix}}}}{\bar{v}^*} \sim \frac{1}{L}\frac{\bar{P}^*}{\bar{P}_y^*} \tag{12}$$

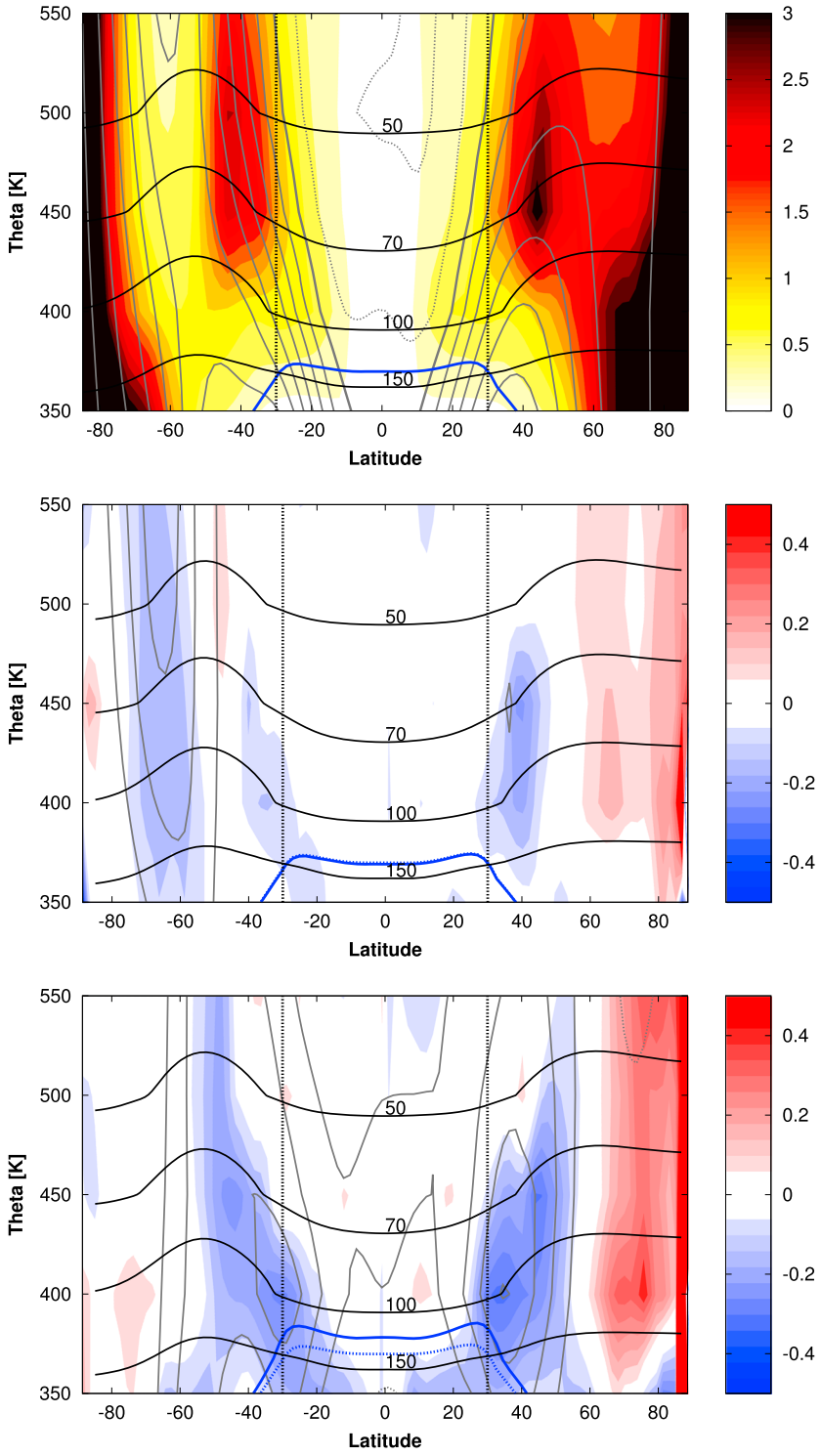

Figure 11. (top) Ratio of mean PV to meridional PV gradient scaled by the Earth radius ($1/R_E PV/\frac{\partial PV}{\partial y}$) for the annual decadal mean from TS1990 together with mean positions of pressure levels (thick black lines), zonal mean zonal wind (gray; contour interval 5 m/s, solid: positive, dotted: negative, thick line: zero) and the tropopause (blue). Relative differences in $PV/\frac{\partial PV}{\partial y}$ for (middle) TS1990-TS1860 and (bottom) TS2050-TS1990 together with differences in zonal mean winds (contour interval 1 m/s, solid: positive, dotted: negative) and the tropopause in TS1990 (dashed blue) and TS1860/TS2050 (solid blue).

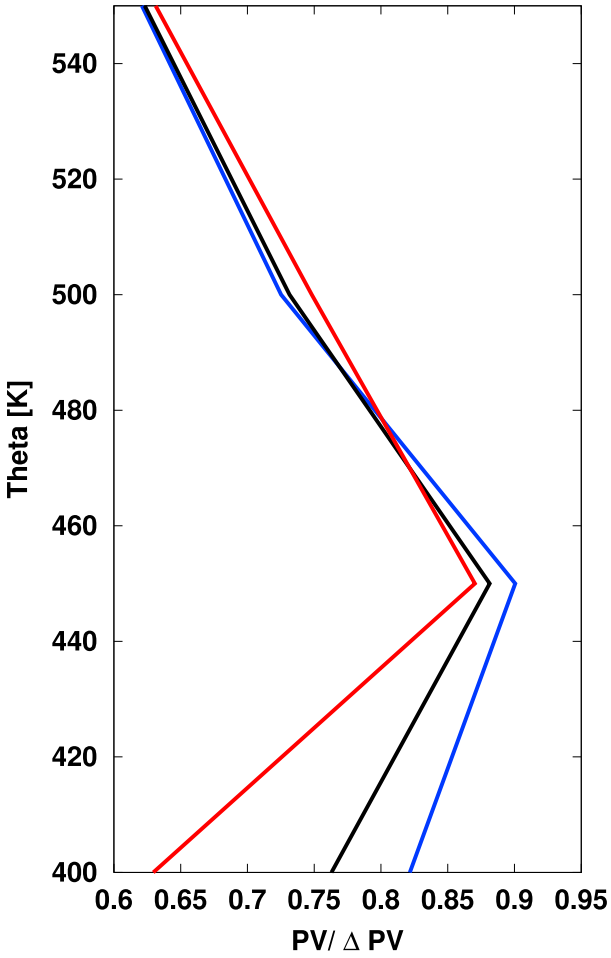

Figure 12. Ratio of tropical mean PV to the gradient extratropical-tropical PV for TS1860 (blue), TS1990 (black), and TS2050 (red).

Thus, the ratio of mean PV to the meridional PV gradient is a measure of the relative role of mixing and mean transport (for a given horizontal mixing length scale). Larger ratios indicate a more important role of mixing, while relatively small values indicate that mean transport dominates. The climatological mean ratio of mean PV to the PV gradient, scaled by the earth radius for the TS1990 simulation is shown in Figure 11 (top). We find elevated ratios between about 30° and 60°N/S above 400 K, consistent with strong wave mixing in the surf zones. The ratio decreases toward the tropics, where the zonal wind approaches zero and wave propagation is largely prohibited. Minima in the ratio at around 60°N/S mark the barrier formed by the polar vortex, in particular in the southern hemisphere. At high latitudes the ratio of mean PV to the PV gradient increases strongly, reflecting that the mean meridional velocity is close to zero here.

The relative changes in the ratio of mean PV to the PV gradient between the TS1860 to the TS1990 simulations, and the TS1990 to TS2050 simulations are shown in Figure 11 (middle and bottom). From 1860 to 1990, the Antarctic polar vortex strengthens, and thus the ratio decreases, as a stronger vortex more strongly suppresses wave mixing. This decrease in mixing is reflected in a stronger gradient in AoA (not shown). From 1860 to 1990, the ratio decreases by about 10–15% at latitudes between about 30 and 50°N/S, and this decrease is even stronger (up to 30%) from 1990 to 2050. This decrease in the relative strength of mixing appears to be associated with the strengthening of the subtropical jets, which are marked by strong PV gradients.

The results of the last section imply that the mixing mass flux between tropics and extratropics changes proportionally to mean meridional transport in the three equilibrium climate states. According to equation (12), we should thus expect that the ratio of mean PV to the PV gradient between tropics and extratropics remains close to constant. As in the TLP model, we set the boundaries between tropics and extratropics at 30°N/S. The horizontal mixing length scale L is then the mean mixing length between tropics and extratropics, and the PV gradient is $\bar{P}_y^* = \Delta\bar{P}^*/L$, where $\Delta\bar{P}^*$ is the extratropical-tropical PV difference. Therefore, the relation of the mixing velocity to the mean meridional velocity across the tropical boundaries can be approximated by the tropical mean PV to the extratropical-tropical PV difference.

This ratio is shown for the three climate states simulated by the GCM in Figure 12. Above 400 K, the ratio differs by less than 3% between the three climate states. At 400 K, the ratio decreases by 8% from 1860 to 1990 and by 17% from 1990 to 2050. This decrease in the PV ratio across 30°N/S is consistent with the decline in $\bar{P}^*/\bar{P}_y^*$ around the subtropical jets shown in Figure 11. Above 400 K, changes in $\bar{P}^*/\bar{P}_y^*$ occur away from the subtropical barrier, so that exchange of air between tropics and extratropics is not affected.

The scaling arguments using PV gradients therefore largely support the results of the last section: Between 450–550 K (i.e., about 65–35 hPa), the relative role of mixing versus mean transport across the subtropical barrier as estimated by the ratio of mean PV to PV gradient remain close to constant, despite changes

in the meridional circulation. However, we found a decrease in the relative role of mixing at 400 K, which might be related to a strengthening of the subtropical jets. We would expect this decrease to be reflected in AoA, in particular since mixing just above the tropopause was found to contribute most to aging by mixing (section 4.2). However, the changes at 400 K appear to be unimportant for the mixing efficiency, which is derived with the TLP model as best fit over the entire lower stratosphere. Note, however, that deviations between the TLP fit with a mixing efficiency of 0.32 and the AoA from the GCM are largest just above the tropopause (see Figure 3).

6. Discussion and Conclusions

The conceptual picture of stratospheric transport consisting of net transport along the residual circulation and modifications by a two-way mass flux ("mixing mass flux") is used widely in stratospheric research [e.g., *Plumb*, 2002]. Here the diagnostic aging by mixing is introduced that quantifies the effects of mixing on age of air. This aging by mixing is obtained by differencing AoA with a hypothetical age that would result from transport along the residual circulation only, the residual circulation transit time (RCTT). Aging by mixing is calculated from global model data, and the processes that lead to aging by mixing are investigated with conceptual model approaches, namely, with a tropical leaky pipe model and a simple Lagrangian random walk model. Above the tropical tropopause, mixing between the tropics and extratropics causes air to recirculate along the residual circulation, thereby enhancing AoA above the level at which mixing occurs. In the lowermost stratosphere AoA is reduced by mixing with tropospheric air, which adds very young air and removes old air from the stratosphere. Using the Lagrangian model, we showed that mixing within the extratropics is necessary to explain the latitudinal distribution of aging by mixing (which maximizes in midlatitudes) but has a negligible (despite nonzero) impact on extratropical mean AoA. Therefore, tropical and extratropical mean AoA profiles from the GCM can be approximated with the tropical leaky pipe model equations, which only consider the effects of mixing across the subtropical barrier.

Decreases of AoA in a future climate are both due to a decrease in RCTT and in aging by mixing, each contributing about half. This result is consistent with *Li et al.* [2012], who examined changes in age spectra and showed that the tail of the spectrum contributes significantly to the future decrease in mean AoA.

Fitting a simple tropical leaky pipe model to AoA from the global model for different climate equilibrium states suggests that the strength of the two-way mixing mass flux is tightly coupled to the net or residual mass flux, so that their ratio (the mixing efficiency) remains close to constant. Thus, the relative aging of air by mixing remains approximately constant. The decrease in absolute aging by mixing is not caused by a decrease in mixing, but by the stronger residual circulation, which leads to faster recirculation. This is again consistent with the decrease in the tail of the spectrum, and in particular with strong correlations of tail decay time scales with the strength of tropical upwelling found by *Li et al.* [2012]. Furthermore, *Li et al.* [2012] found that mixing strength (estimated as equivalent length from N_2O) increases proportionally with tropical upwelling, consistent with our finding of a constant mixing efficiency.

We further verified the result of a nearly constant mixing efficiency by evaluating the ratio between mean PV to the PV gradient between tropics and extratropics, which is a measure of the relative roles of mixing versus mean horizontal transport. In most of the lower stratosphere, this ratio is found to remain close to constant between the climate states, consistent with a constant mixing efficiency. However, just above the tropopause (at 400 K) the ratio of mean PV to PV gradients decreases, indicating that mixing fluxes decrease relative to mean transport. An increase in the strength of the subtropical jets might cause this decrease in mixing relative to mean transport. The causes for the decrease in the relative strength of mixing at 400 K indicated by the PV analysis, along with deviations in the TLP model fits at these levels remain to be identified. It might indicate a different regime of transport and mixing in the shallow branch. However, note that both the TLP model and the PV scaling arguments rely on simplified assumptions. Independent measures of mixing like the effective diffusivity [*Allen and Nakamura*, 2001], or Lagrangian measures, have to be used to verify the relation of the two-way mass flux to residual transport (as shown in *Li et al.* [2012]). Furthermore, it is questionable whether the tight coupling between residual transport and mixing also holds at higher altitudes where gravity waves play a larger role in driving the residual circulation, since gravity waves mostly cause two-way mixing in the vertical [*Grygalashvyly et al.*, 2012] but do not primarily alter the PV distribution along isentropes in the same manner as Rossby waves.

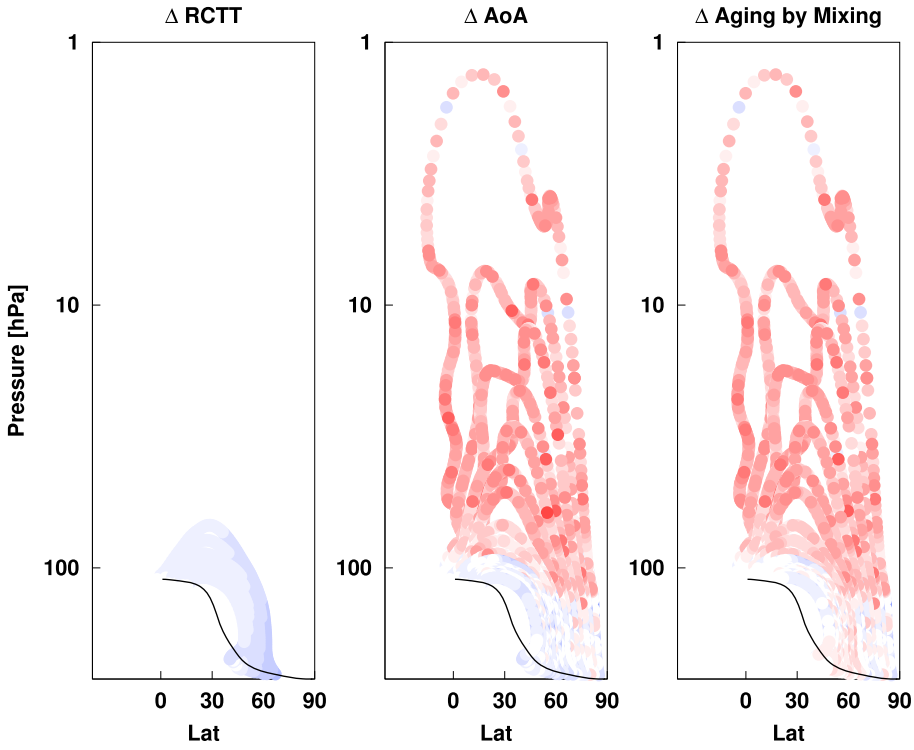

Figure 13. Idealized experiment with the Lagrangian random walk model resembling an intensification of the shallow branch only. Advection along the shallow branch trajectories is sped up (as seen in the difference to the base case in RCTT, left) and the mixing fraction is enhanced in the lower part so that the mixing efficiency remains constant. The resulting change in AoA and aging by mixing compared to the base case is shown in the middle and right panels. Color shading as in Figure 2.

The modeled strength of the two-way mass flux depends on stirring by large-scale winds but also on the advection scheme and representation of (subgrid scale) diffusion. Therefore, the two-way mass flux likely differs between models, even if the large-scale dynamics are similar, resulting in differences in the mixing efficiency. The separation of AoA into RCTT and aging by mixing and the comparison of the relative aging by mixing (or of the mixing efficiency) between models might provide a helpful tool to identify causes for model deficits in the simulation of AoA that are widely found in state-of-the art global models [see *SPARC-CCMVal*, 2010, chapter 5].

An as yet unresolved puzzle is the discrepancy between the few available observational records of the temporal development of AoA over the last decades and modeled changes in AoA. Global models simulate an increase in the BDC and associated decrease in AoA over the last decades and in the future [*Butchart et al.*, 2010]. The longest available time series of AoA derived from measurements of SF_6 shows no significant change in AoA at northern midlatitudes at around 25 km [*Engel et al.*, 2009]. This results is backed up by AoA records derived from satellite observations of SF_6 [*Stiller et al.*, 2012], and by AoA time series calculated from reanalysis [*Diallo et al.*, 2012]. The latter study suggests that AoA decreased in the lower stratosphere but increased above about 20 to 25 km over the period 1989–2010. On the basis of tracer measurements in the lowermost stratosphere and residual circulation transit time calculations, *Bönisch et al.* [2011] suggested that structural changes in the BDC occurred over the last decades, with an intensification of the shallow branch, while the deep branch remained unchanged.

How structural changes in the residual circulation would modify AoA can be illustrated with the Lagrangian random walk model used in this study. The Lagrangian model allows for a separation of the shallow and deep branch, and the response to a hypothetical speed up of the shallow branch with associated increases in the mixing fraction (given a constant mixing efficiency) are shown in Figure 13. The faster circulation in the lower stratosphere causes decreases in AoA there, but above, AoA increases. This increase is due to aging by mixing, which, as discussed above, results from an enhanced mixing mass flux in the lower stratosphere. This simple experiment shows that despite the coupling of mixing and the residual circulation, mixing can

act to either amplify or dampen residual circulation changes, depending on the relative location in the atmosphere with respect to the circulation changes. The AoA changes due to a shallow branch enhancement found in the Lagrangian model experiment are consistent with the findings by *Bönisch et al.* [2011] and the AoA trend pattern in reanalysis data presented by *Diallo et al.* [2012].

Appendix A: Parameter Settings in the Lagrangian Random Walk Model

The simple Lagrangian random walk model used in section 4.2 advects air parcels along trajectories that are calculated from residual velocities. Two-way mixing is realized by exchanging a certain fraction of air parcels between or within different groups, namely, the tropics (region of upwelling) and the extratropics (region of downwelling). The air parcels are randomly selected according to an uniform distribution. The points where this parcel exchange (= mixing) is performed are located on the intersections of trajectories with selected isentropic levels. Several different parameters need to be chosen (1) Number of trajectories (Ntraj), (2) Number of theta levels on which mixing is performed, (3) The fraction of air parcels that are exchanged (mixing fraction μ).

For the "base case", we use monthly mean residual velocities to calculate 20 trajectories that are initialized at the tropopause between 40 and 85°N, and 20 mixing levels between 340 to 2000 K.

The fraction of mass exchange representing mixing within the extratropics and within the tropics is set to 0.25. The choice of the fraction of air exchange between the tropics and the extratropics ($\mu_{\mathrm{TrEx}}(z)$) is anticipated to be based on physical principles. In particular, we assume that the net mass flux from the tropics to the extratropics is proportional to the mixing mass flux, as suggested by the results of section 5. Thus,

$$\epsilon \times \mathrm{massflux}_{net} = \mathrm{massflux}_{\mathrm{mix}} \tag{A1}$$

where ϵ is the mixing efficiency as defined in the TLP model. The net mass flux from the tropics to the extratropics in one hemisphere can be expressed as

$$\mathrm{massflux}_{\mathrm{net}} = -\frac{1}{2}\frac{\partial}{\partial z}\left(M_T w_T\right) = -\frac{1}{2}\frac{\partial}{\partial z}\left(M_T(z_T)\exp(-\frac{z-z_T}{H})w_T(z)\right) \tag{A2}$$

assuming an increase of the mass M_T with height according to $M_T(z) = M_T(z_T)\exp(-\frac{z-z_T}{H})$, where $M_T(z_T)$ is the mass at the tropical tropopause. The mixing mass flux in the Lagrangian model can be written as

$$\mathrm{massflux}_{\mathrm{mix}} = \mu_{\mathrm{TrEx}}(z) \times 100 m_0 N(z)\frac{1}{\Delta t} \tag{A3}$$

where m_0 is the mass of one air parcel that travels along the trajectories, and N is the number of trajectories that take part in the mixing process at level z. Δt is the time step of the Lagrangian model, here 5 days.

Combining these equations, one obtains for the mixing fraction $\mu_{\mathrm{TrEx}}(z)$:

$$\mu_{\mathrm{TrEx}}(z) = -\epsilon\frac{0.5M_T(z_T)}{100m_0N(z)} \times \Delta t \times \frac{\partial}{\partial z}\left(\exp(-\frac{z-z_T}{H})w_T(z)\right). \tag{A4}$$

Given that the total mass at the tropical tropopause equals the mass of the air parcels that are located at this level in the Lagrangian model, i.e., $2 \times 100 \times m_0 \times N(z_T)$, we can write

$$\mu_{\mathrm{TrEx}}(z) = -\epsilon\frac{N(z_T)}{N(z)} \times \Delta t \times \frac{\partial}{\partial z}\left(\exp(-\frac{z-z_T}{H})w_T(z)\right). \tag{A5}$$

Since mixing is performed on a finite number of height levels, μ needs to be scaled to represent mixing over the entire layer it represents. Thus, the fraction of parcels mixed (exchanged) at level z is multiplied by the mass within the entire layer divided by the mass at level z: $\mu_{\mathrm{TrEx}}(\Delta z) = \mu_{\mathrm{TrEx}}(z) \times N(\Delta z)/N(z)$. This ensures robust results with respect to the location and number of mixing levels. As shown in Table A1, global mean age simulated with additional levels (37 instead of 20 used in the base case) differs by less than 1% from the base case.

The tropical vertical velocity w_T used here is the tropical mean (30°N/S) $\bar{w}^*$ taken from the GCM data. The mixing efficiency ϵ can be derived from the relation of AoA and RCTT in the GCM by using the TLP model (see section 4.1). For the latitude band of 30°N–30°S, the TLP fit gives $\epsilon \approx 0.3$. This value gives good

Table A1. Global Mean (GM) AoA, RCTTs, and Aging by Mixing (in Years) as Simulated in the Lagrangian Random Walk Model for the Base Case and Sensitivities to the Mixing Efficiency ϵ, the Number of Isentropic Mixing Levels, and the Number of Trajectories Used

		ϵ		Θ Level	Ntraj	
	Base	0.4	0.2	37	10	40
GM RCTT	1.25	1.25	1.25	1.25	1.39	1.21
GM AoA	1.69	1.91	1.50	1.68	1.95	1.58
GM A_{Mix}	0.44	0.66	0.25	0.43	0.56	0.37

agreement between the Lagrangian calculations and the AoA profiles from the GCM (see Figure 6). Calculations with modified values of ϵ show that AoA increases in the global mean for higher ϵ, as expected (see Table A1).

When using a different number of trajectories, different global mean values of RCTTs are obtained, as listed in Table A1. Applying mixing in the same manner to those cases results in an increase in global mean AoA in all cases, and tropical and extratropical profiles show good agreement (not shown). However, in the case of using 10 trajectories, AoA increases by 40% due to mixing, while when using 40 trajectories the increase lies around 30%. The base case gave a 35% increase. Thus, the simple Lagrangian model is somewhat sensitive to the choice of the trajectory set, and it should be regarded as a conceptual model used to highlight different effects rather than a quantitative model.

Acknowledgments
This study was funded by the Deutsche Forschungsgemeinschaft (DFG) through the DFG-research group SHARP (Stratospheric Change And its Role for climate Prediction). We thank M. Dameris, V. Grewe, and M. Abalos for discussion and comments, as well as R.A. Plumb and the two anonymous reviewers for very valuable comments on the manuscript. T.B. acknowledges funding through the Climate and Large-Scale Dynamics Program of the U.S. National Science Foundation.

References

Allen, D. R., and N. Nakamura (2001), A seasonal climatology of effective diffusivity in the stratosphere, *J. Geophys. Res.*, *106*, 7917–7936, doi:10.1029/2000JD900717.
Andrews, D., J. Holton, and C. Leovy (1987), *Middle Atmosphere Dynamics*, Academic Press, San Diego, Calif.
Austin, J., and F. Li (2006), On the relationship between the strength of the Brewer-Dobson circulation and the age of stratospheric air, *Geophys. Res. Lett.*, *33*, L17807, doi:10.1029/2006GL026867.
Birner, T., and H. Bönisch (2011), Residual circulation trajectories and transit times into the extratropical lowermost stratosphere, *Atmos. Chem. Phys.*, *11*(7), 817–827, doi:10.5194/acp-11-817-2011.
Bönisch, H., A. Engel, J. Curtius, T. Birner, and P. Hoor (2009), Quantifying transport into the lowermost stratosphere using simultaneous in-situ measurements of SF6 and CO_2, *Atmos. Chem. Phys.*, *9*, 5905–5919, doi:10.5194/acp-9-5905-2009.
Bönisch, H., A. Engel, T. Birner, P. Hoor, D. W. Tarasick, and E. A. Ray (2011), On the structural changes in the Brewer-Dobson circulation after 2000, *Atmos. Chem. Phys.*, *11*, 3937–3948, doi:10.5194/acp-11-3937-2011.
Bunzel, F., and H. Schmidt (2013), The Brewer-Dobson circulation in a changing climate: Impact of the model configuration, *J. Atmos. Sci.*, *70*, 1437–1455, doi:10.1175/JAS-D-12-0215.1.
Butchart, N. (2014), The Brewer-Dobson circulation, *Rev. Geophys.*, doi:10.1002/2013RG000448.
Butchart, N., et al. (2010), Chemistry-climate model simulations of twenty-first century stratospheric climate and circulation changes, *J. Clim.*, *23*, 5349–5374, doi:10.1175/2010JCLI3404.1.
Calvo, N., and R. R. Garcia (2009), Wave forcing of the tropical upwelling in the lower stratosphere under increasing concentrations of greenhouse gases, *J. Atmos. Sci.*, *66*, 3184–3196, doi:10.1175/2009JAS3085.1.
Diallo, M., B. Legras, and A. Chédin (2012), Age of stratospheric air in the ERA-Interim, *Atmos. Chem. Phys.*, *12*, 12,133–12,154, doi:10.5194/acp-12-12133-2012.
Engel, A., et al. (2009), Age of stratospheric air unchanged within uncertainties over the past 30 years, *Nat. Geosci.*, *2*, 28–31, doi:10.1038/ngeo388.
Garcia, R., and W. Randel (2008), Acceleration of the Brewer-Dobson circulation due to increases in greenhouse gases, *J. Atmos. Sci.*, *65*, 2731–2739.
Grygalashvyly, M., E. Becker, and G. R. Sonnemann (2012), Gravity wave mixing and effective diffusivity for minor chemical constituents in the mesosphere/lower thermosphere, *Space Sci. Rev.*, *168*, 333–362, doi:10.1007/s11214-011-9857-x.
Hall, T. M., and R. Plumb (1994), Age as a diagnostic of stratospheric transport, *J. Geophys. Res.*, *99*, 1059–1070.
Haynes, P., and E. Shuckburgh (2000), Effective diffusivity as a diagnostic of atmospheric transport: 1. Stratosphere, *J. Geophys. Res.*, *105*, 22,777–22,794, doi:10.1029/2000JD900093.
Haynes, P., C. Marks, M. McIntyre, T. Shepherd, and K. Shine (1991), On the "downward control" of extratropical diabatic circulations by eddy-induced mean zonal forces, *J. Atmos. Sci.*, *48*(4), 651–678.
Li, F., D. Waugh, A. R. Douglass, P. A. Newman, S. E. Strahan, J. Ma, J. E. Nielsen, and Q. Liang (2012), Long-term changes in stratospheric age spectra in the 21st century in the Goddard Earth Observing System Chemistry-Climate Model (GEOSCCM), *J. Geophys. Res.*, *117*, D20119, doi:10.1029/2012JD017905.
Marsland, S. (2003), The Max-Planck-Institute global ocean/sea ice model with orthogonal curvilinear coordinates, *Ocean Modell.*, *5*, 91–127, doi:10.1016/S1463-5003(02)00015-X.
McIntyre, M., and T. Palmer (1984), The "surf zone" in the stratosphere, *J. Atmos. Terr. Phys.*, *46*(9), 825–849.
McLandress, C., and T. G. Shepherd (2009), Simulated anthropogenic changes in the Brewer-Dobson circulation, including its extension to high latitudes, *J. Clim.*, *22*, 1516–1540, doi:10.1175/2008JCLI2679.1.
Nakicenovic, N., and R. Swart (2000), Special report on emissions scenarios, *Tech. Rep.*, Cambridge Univ. Press.
Neu, J. L., and R. A. Plumb (1999), Age of air in a "leaky pipe" model of stratospheric transport, *J. Geophys. Res.*, *104*(D16), 243–255, doi:10.1029/1999JD900251.
Oberländer, S., U. Langematz, and S. Meul (2013), Unraveling impact factors for future changes in the Brewer-Dobson circulation, *J. Geophys. Res. Atmos.*, *118*, 10,296–10,312, doi:10.1002/jgrd.50775.
Okamoto, K., K. Sato, and H. Akiyoshi (2011), A study on the formation and trend of the Brewer-Dobson circulation, *J. Geophys. Res.*, *116*, D10117, doi:10.1029/2010JD014953.
Plumb, R. (2002), Stratospheric transport, *J. Meteorol. Soc. Jpn.*, *80*, 793–809.
Randel, W., J. Gille, A. Roche, J. Kumer, J. Mergenthaler, J. Waters, E. Fishbein, and W. Lahoz (1993), Stratospheric transport from the tropics to middle latitudes by planetary-wave mixing, *Nature*, *365*, 533–535.

Ray, E. A., et al. (2010), Evidence for changes in stratospheric transport and mixing over the past three decades based on multiple datasets and tropical leaky pipe analysis, *J. Geophys. Res.*, *115*, D21304, doi:10.1029/2010JD014206.
Röckner, E., et al. (2003), The atmospheric general circulation model ECHAM 5. Part I: Model description, *Tech. Rep.*, Max Planck Institute for Meteorology Rep. 349.
Shepherd, T., and C. McLandress (2011), A robust mechanism for strengthening of the Brewer-Dobson circulation in response to climate change: Critical-layer control of subtropical wave breaking, *J. Atmos. Sci.*, *68*, 784–797.
Shepherd, T. G. (2007), Transport in the middle atmosphere, *J. Meteorol. Soc. Jpn.*, *85B*, 165–191.
Shuckburgh, E., and P. Haynes (2003), Diagnosing transport and mixing using a tracer-based coordinate system, *Phys. Fluids*, *15*, 3342–3357, doi:10.1063/1.1610471.
SPARC-CCMVal (2010), Sparc report on the evaluation of chemistry-climate models, *Tech. Rep., SPARC Rep. 5, WCRP-132, WMO/TD-1526*, edited by V. Eyring, T. G. Shepherd, and D. W. Waugh.
Sparling, L. C., J. A. Kettleborough, P. H. Haynes, M. E. Mcintyre, J. E. Rosenfield, M. R. Schoeberl, and P. A. Newman (1997), Diabatic cross-isentropicdispersion in the lower stratosphere, *J. Geophys. Res.*, *102*, 25,817–25,829.
Stevens, B., et al. (2013), Atmospheric component of the MPI-M Earth system model: ECHAM6, *J. Adv. Model. Earth Syst.*, *5*, 146–172, doi:10.1002/jame.20015.
Stiller, G. P., et al. (2012), Observed temporal evolution of global mean age of stratospheric air for the 2002 to 2010 period, *Atmos. Chem. Phys.*, *12*, 3311–3331, doi:10.5194/acp-12-3311-2012.
Strahan, S. E., M. R. Schoeberl, and S. D. Steenrod (2009), The impact of tropical recirculation of polar composition, *Atmos. Chem. Phys.*, *9*, 2471–2480, doi:10.5194/acp-9-2471-2009.
Trepte, C. R., and M. H. Hitchman (1992), Tropical stratospheric circulation deduced from satellite aerosol data, *Nature*, *355*, 626–628.
Vuuren, D. P., et al. (2011), The representative concentration pathways: An overview, *Clim. Change*, *109*, 5–31.